European Journal of Medicinal Chemistry 96 (2015) 259–268

Contents lists available at ScienceDirect

European Journal of Medicinal Chemistry

journal homepage: http://www.elsevier.com/locate/ejmech

Original article

Identification of an anti-inflammatory derivative with anti-cancer potential: The impact of each of its structural components on inflammatory responses in macrophages and bladder cancer cells

Jovane Hamelin-Morrissette [a, 1], Suzie Cloutier [b, 1], Julie Girouard [a], Denise Belgorosky [c], Ana María Eiján [c], Jean Legault [d], Carlos Reyes-Moreno [a, *], Gervais Bérubé [b, *]

[a] Département de Biologie Médicale et, Canada
[b] Département de Chimie, Biochimie et Physique, Université du Québec à Trois-Rivières, C.P. 500, Trois-Rivières, Québec G9A 5H7, Canada
[c] Instituto de Oncologia "Ángel H. Roffo" Área Investigación, Ciudad de Buenos Aires, C1417DTB, Argentina
[d] Département des Sciences Fondamentales, Université du Québec à Chicoutimi, 555 boulevard de l'Université, Chicoutimi, Québec G7H 2B1, Canada

ARTICLE INFO

Article history:
Received 29 October 2014
Received in revised form
9 April 2015
Accepted 10 April 2015
Available online 13 April 2015

Keywords:
Bladder cancer
Inflammation
Interferon gamma
Interleukine 6
Nitric oxide
STAT pathway

ABSTRACT

Inflammation plays a crucial role in many types of cancer and is known to be involved in their initiation and promotion. As such, it is presently recognized as an important risk factor for several types of cancers such as bladder, prostate and breast cancers. The discovery of novel anti-inflammatory compounds can have a huge implication not only for the treatment of cancer but also as preventive and protective treatment modalities. We have recently identified a new compound (**1**) that presents interesting anti-inflammatory activity. In order to better understand its biological action, we have divided the molecule in its basic components and verified their respective contribution towards the anti-inflammatory response of the whole molecule. We have discovered that only the combination of the maleimide function together with the *tert*-butyloxycarbonylhydrazinamide function lead to important anti-inflammatory properties. The main derivative **1** can decrease the activating effects of INFγ or IL6 on human (hMϕs) macrophages by 38% or by 64% at a concentration of 10 μM as indicated by a decrease of STAT1 or STAT3 activation. The expression of pro-inflammatory markers CD40 and MHCII in INFγ stimulated hMϕs were reduced by 87% and 49%, respectively with a 3 h pretreatment of **1** at 10 μM. The cell motility assay revealed that **1** at 10 μM can reduce relative cell motility induced by IL6 by 92% in comparison with the untreated control hMϕ monolayers. Compound **1** reduced by 91% the inflammatory response induced by the cytokines (INFγ + TNFα) in the macrophage-like J774A.1 cells at a concentration of 25 μM, as measured by the detection of NO production with the Griess reagent. Furthermore, upon removal of the *tert*-butyloxycarbonyl protective group the unprotected derivative as a hydrochloride salt (**1A**) retains interesting anti-inflammatory activity and was found to be less toxic than the parent compound (**1**).

1. Introduction

Bladder cancer (BCa) is the second most common tumor of urogenital tract. In fact, it is the seventh most frequent cancer in the world and the fourth in developed countries [1]. In Canada, BCa ranked fifth among all cancer cases diagnosed in the Canadian population with about 8000 new cases diagnosed during 2014 [2]. Most of detectable BCa tumors are initially non-muscle-invasive at diagnosis and are generally curable by means of chirurgical resection. For BCa patients with non-muscle-invasive tumors, intravesical immunotherapy with the immunomodulator Bacillus Calmette-Guerin (BCG) or chemotherapeutic agents is recommended for reducing the risk of tumor recurrence [3]. However, the current treatments are still far from satisfactory due to low

Abbreviations list: BCa, bladder cancer; macrophage, Mϕ; NO, nitric oxide.

* Corresponding authors.
E-mail addresses: jovane.hamelin@outlook.com (J. Hamelin-Morrissette), Suzie.Cloutier@uqtr.ca (S. Cloutier), Julie.Girouard@uqtr.ca (J. Girouard), d_belgo@hotmail.com (D. Belgorosky), anamariaeijan@fibertel.com.ar (A.M. Eiján), jean.legault@uqac.ca (J. Legault), Carlos.Reyes-Moreno@uqtr.ca (C. Reyes-Moreno), Gervais.Berube@uqtr.ca (G. Bérubé).

[1] These authors contributed equally to this work.

http://dx.doi.org/10.1016/j.ejmech.2015.04.026
0223-5234/

response rate and/or severe side effects [4]. In fact, it is estimated that about 27–30% of new cases diagnosed will die from that disease due to recurrent tumors exhibiting a lethal phenotype characterized by high histological grade and muscle invasion [1,2].

At present, as the mechanisms of acquisition of highly malignant phenotype of BCa tumors are not yet well understood, very few therapeutic alternatives have been proposed and tested in the clinic. Nevertheless, compelling data actually suggest that chronic inflammation acts as an important mediator of human carcinogenesis and cancer disease progression [5–10]. In the case of BCa, evolution into different stages of cancer development is strongly associated with episodes of chronic inflammation caused by tobacco smoke, urinary tract infections or chronic cystitis [11–13]. For instance, higher levels of pro-inflammatory cytokines and tumor-infiltrating macrophages (Mϕs) were found to be associated with more aggressive tumors, low responsiveness to intravesical BCG therapy, and poor prognosis [5–7,14–18]. In our recent studies, *in vitro* models of functional interactions between human cancer cells and two different subtypes of human Mϕs, pro-inflammatory Mϕ-1 and anti-inflammatory Mϕ-2, were developed in an attempt to investigate the role of polarized Mϕs in human cancer cell behavior changes [19,20]. Our findings that both types of Mϕs can regulate tumor cell survival and invasion further support the idea that, via alterations in the expression of inflammatory mediators and inflammatory cell function, the inflammatory microenvironment may contribute to the development of a highly malignant phenotype of tumors *in vivo* [19,20].

Among the major regulator of systemic and local inflammation, the cytokines tumor necrosis factor alpha (TNFα) and interleukin 6 (IL6) have been shown to promote BCa development [5]. In theory, TNFα and IL6 exert pro-tumoral effects on tumor cells through activation of the transcription factors nuclear factor kappa B (NFκB) and signal transducer and activator of transcription 3 (STAT3), respectively [21]. The signaling pathways TNFα/NFκB and IL6/STAT3 were identified as the main factors that transform the intratumoral leukocytes into pro-tumor cells [5]. Such functional phenotype control is critical to prevent tumor immune surveillance and instead, to turn away the responses of adaptive and innate immune cells toward the promotion of highly invasive, lethal forms of BCa.

Nitric oxide (NO), another important component of the inflammatory response, is often deregulated and associated with numerous types of malignancies, including BCa [22–26]. It is known that NO can have dichotomous effects on tumor growth, depending on its concentration, time of exposure and tumor microenvironment. These dual effects of NO on cancer arise from its ability to regulate different events such as induction of DNA damage, suppression of DNA repair enzymes, posttranslational modifications of proteins, enhancement of cell proliferation, inhibition of apoptosis and antitumor immunity [23–25]. It is known that one of the isoforms of the enzyme that produces NO (inducible nitric oxide synthase (iNOS)) is not expressed in normal bladder, but is detected in approximately 50% of bladder tumors, being a poor prognosis factor associated with tumor invasion in patients with BCa [26]. Treatment with an inhibitor of NO production in a murine model, inhibited properties *in vitro* and *in vivo*, related to tumor growth, progression, and viability [22]. Among anticancer strategies, the modulation of NO production for therapeutic benefit has gained interest over the past decade [23,27].

Considering the critical functions of inflammatory mediators in BCa growth, dissemination and resistance to cell death, they represent potential drug targets to improve the efficacy of immunotherapy and chemotherapy agents. The use of chemopreventive agents against inflammatory mediators or key transcription factors involved in the inflammatory proteins expression might thus be a promising approach to decrease cancer development [6,21,23,27,28].

Recently, it was reported that veratric acid, a natural benzoic acid derivative, possesses anti-oxidant, anti-inflammation and blood pressure-lowering effects [29]. Based on the latter study, it was decided to screen a series of benzoic acid analogs made in our laboratory for their potential anti-inflammatory activity. It was discovered that a maleimide-hydrazinecarboxylic acid *tert*-butyl ester derivative possesses good anti-inflammatory properties. This compound was an important intermediate for the construct of heterobifunctional cross-linking reagents allowing the synthesis of doxorubicin-monoclonal antibody immunoconjugates [30,31]. Hence, in order to better understand its unsuspected biological anti-inflammatory action, the molecule was divided into its various components that were individually tested on NO production in bladder cancer cells (MB49-I) along with the product of interest. This study aims at establishing the possible repurposing to this molecule as an anti-inflammatory. This communication reports the synthesis and biological properties of this new anti-inflammatory compound (**1**), its unprotected analog (**1A**) and that of its various structural components (see Fig. 1).

2. Results and discussion

2.1. Chemistry

Using *para*-amino benzoic acid (**2**) as the starting material derivative **1** was made in a three-step reaction sequence (Scheme 1) [30]. *Para*-amino benzoic acid (**2** or **PABA**) was first reacted with maleic anhydride (**MA**) in dry acetone to give the diacid (**3**) with 90% yield. Cyclisation to form the maleimide was accomplished with acetic anhydride and sodium acetate to give compound **4** with 89% yield after hydrolysis of the mixed anhydride intermediate with water. Finally, activation of acid **4** with *iso*-butyl chloroformate in the presence of pyridine was done followed by treatment with *tert*-butyl carbazate gave the desired anti-inflammatory derivative **1** with 54% yield. Deprotection of **1** with hydrochloric acid in ether gave the hydrochloride salt **1A** with 46% yield after recrystallization.

The left and right hands of derivative **1** were also synthesized in order to assess the respective contribution of the remaining functional group towards the observed anti-inflammatory activity. The left hand of **1** was prepared in a two-step reaction sequence from aniline (**5**). The reaction of aniline (**5**) with **MA** followed by cyclisation of the amido-acid intermediate gave the desired maleimide **7** in about 38% overall yield. The right hand of **1** was also prepared in a single step form benzoic acid upon activation with *iso*-butyl chloroformate followed by treatment with *tert*-butyl carbazate to yield compound **9** in 48% yield. Of note, these reactions were not optimized as derivatives **7** and **9** were only needed in small quantities to assess their anti-inflammatory properties in comparison to **1** and **1A**. The compounds were characterized by their respective infrared (IR), nuclear magnetic resonance spectroscopy (proton and carbon NMR) and by high resolution mass analysis.

2.2. Evaluation of anti-inflammatory properties in activated macrophages

This set of experiments were planned to investigate whether the main two derivatives **1** and **1A** have the ability to modulate the activating effects of potent pro-inflammatory cytokines, namely INFγ, TNFα, and IL6, on the behavior of human (hMϕs) and murine (mMϕs) macrophages. IFNγ, through the activation of the transcription factor signal transducer and activator of transcription 1 (STAT1), is known to induce the expression of several pro-inflammatory genes in Mϕs, such as the cytokines TNFα and IL6, and the cell surface receptors cluster of differentiation 40 (CD40)

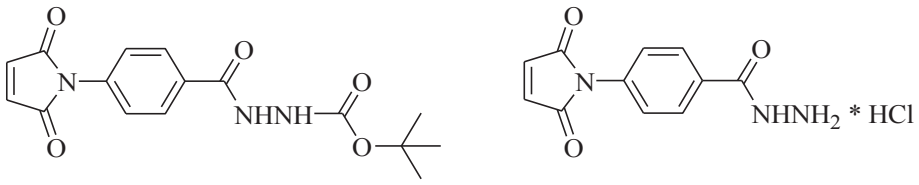

Fig. 1. Molecular structure of *N*′-[4-(2,5-dioxo-2,5-dihydro-pyrrol-1-yl)-benzoyl]-hydrazinecarboxylic acid *tert*-butyl ester (**1**) and of 4-(2,5-dioxo-2,5-dihydro-pyrrol-1-yl)-benzoic acid hydrazide hydrochloride (or 4-maleimidbenzoic acid hydrazide hydrochloride) (**1A**).

and the major histocompatibility complex II (MHC-II) [32]. The cytokine IL6 is a key regulator of systemic and local inflammation [33,34]. Functionally, IL6 mediates its effects through the binding of IL6 receptor subunits IL6R and gp130 which leads to the activation of STAT3 [35]. Activation of the IL6/STAT3 signaling pathway is critical to Mϕ migration and differentiation [36]. On the other hand, TNFα and IFNγ are considered as the most important cytokines involved in NO production by mouse Mϕs [37].

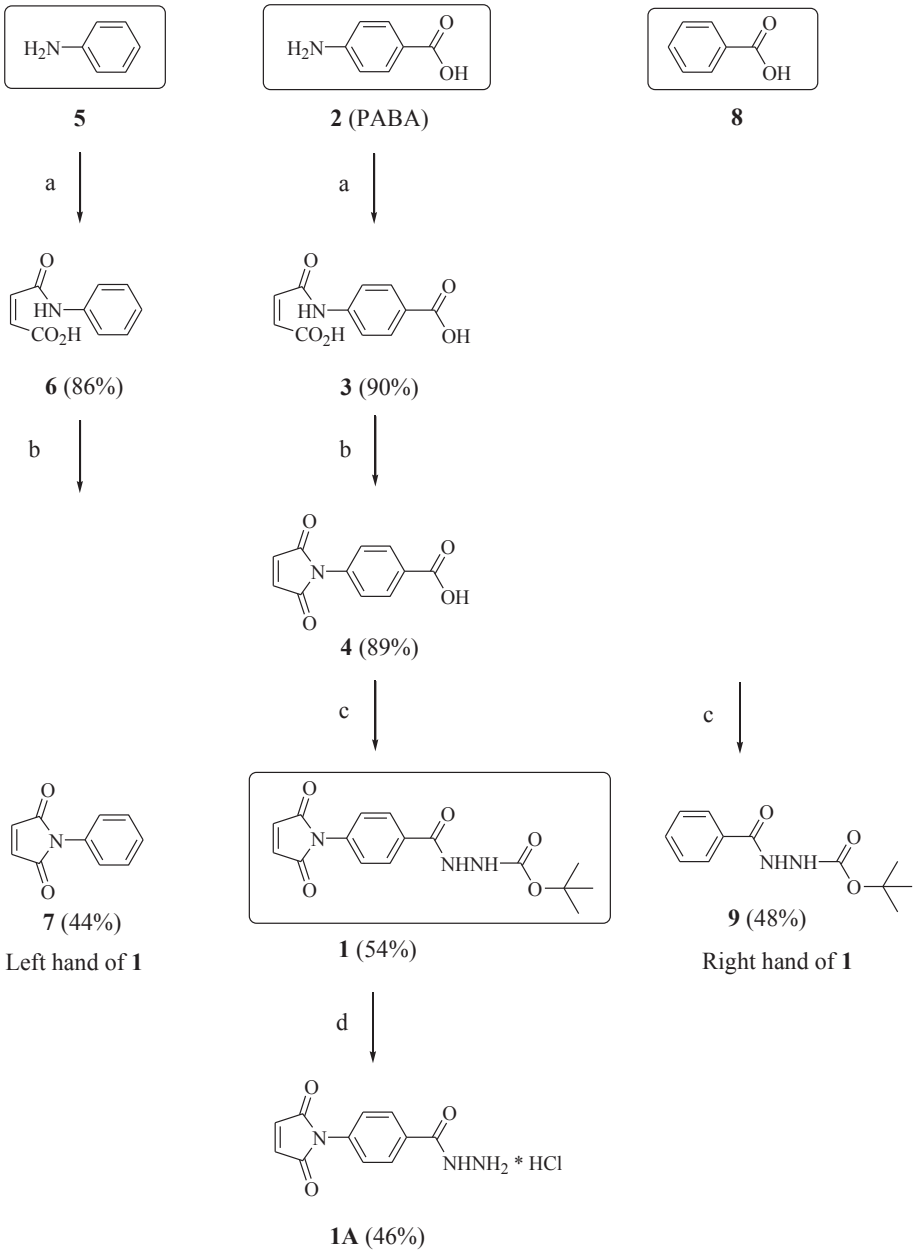

Scheme 1. Reagents and conditions: a) Maleic anhydride (**MA**), dry acetone, methanol, 22 °C, 1 h; b) 1) Ac_2O, AcONa, 50 °C, 2 h; 2) H_2O, 70 °C, 2 h; c) 1) *iso*-butyl chloroformate, Et_3N, CH_2Cl_2, 0 °C, 1 h and 22 °C, 1 h; 2) *tert*-butyl carbazate, CH_2Cl_2, 22 °C, 12 h; d) HCl, dioxane, 22 °C, 5 h.

Fig. 2a shows representative activation status of STAT1 by IFNγ and STAT3 by IL6 in hMϕs pretreated for 30 min with derivatives **1A** and **1**. hMϕs express low basal levels of pSTAT1 and pSTAT3 (t = 0 min) when pretreated with derivatives **1A** or **1** (Fig. 2a). Very little or no variation in total STAT1 and STAT3 expression was observed, irrespective of the treatments. As expected, IFNγ activates STAT1, the levels of pSTAT1 being increased with IFNγ at t = 30 min (Fig. 2b). These increased effects in pSTAT1 were efficiently reduced when hMϕs were pretreated with **1A** (from 14.8 folds to 12.4 folds at 10 μM, and 5.1 folds at 50 μM) and even more with **1** (from 9.9 folds to 6.1 folds at 10 μM, and 2.8 folds at 50 μM). Similar to pSTAT1 by IFNγ, the induction of pSTAT3 by IL6 was significantly reduced when hMϕs were pretreated with **1A** (from 23.1 folds to 19.7 folds at 10 μM, and 14.2 folds at 50 μM) and even more with **1** (from 32.9 folds to 11.9 folds at 10 μM, and 4.9 folds at 50 μM).

To further investigate the influence of derivatives **1** and **1A** on the biological responses induced by inflammatory mediators in hMϕs, two set of experiments were designed to evaluate the expression level of the pro-inflammatory markers CD40 and MHC-II in IFNγ-stimulated hMϕs, by flow cytometry, and cell motility in IL6-stimulated hMϕs, by the scratch wound healing assay. Consistently with the pro-inflammatory role of IFNγ, Mϕ CD40 and MHC-II expressions were enhanced by 16.7 folds and 15.3 folds, respectively (Fig. 3). However, the rise in CD40 expression in IFNγ-activated Mϕs was blocked when they were pretreated with **1A** (9.5 folds) and even more with **1** (2.2 folds). For MHC-II, the expression inductions were reduced to 11.8 folds with **1A** and 7.8 folds with **1**. Scratch assays were performed to further demonstrate the deactivating effects of derivatives **1** and **1A** on IL6-activated hMϕs (Fig. 4a). We found that stimulation with exogenous IL6 for 48 h significantly enhanced hMϕ motility, the ratio of motile cells being increased up to 177% compared with control cells (Fig. 4b). However, the stimulatory effect of IL6 on cell motility was significantly blocked when hMϕs were pretreated with derivatives **1A** and **1**; the relative number of motile cells being decreased to 53.7% of control with **1A**, and to 13.5% of control with **1** (Fig. 4b).

Finally, anti-inflammatory activity was assessed by measuring NO production in mMϕs stimulated by two potent pro-inflammatory signals, INFγ and TNFα, and using the Griess reaction method according to the published procedure [22]. In brief, the NO produced by the cells is converted into nitrite ion (NO_2^-). The latter is reacted with the Griess reagent to form an azo dye that can be spectrophotometrically quantitated based on its absorbance at 548 nm. As shown in Fig. 5, in response to combined INFγ + TNFα activation, the production of NO were increased by 8.7 folds (from 7 ± 3 μM in unstimulated cells up to 61 ± 9 μM in stimulated cells). However, when mMϕs were activated after pretreatment with derivatives **1A** and **1** both at a concentration of 10 μM, NO production was only induced by 6.6 folds (45.9 μM) and 4.7 folds (32.8 μM), respectively. Also, in the presence of derivatives **1A** and **1** at a concentration of 50 μM, the induction of NO production was respectively reduced to 2.7 folds (18.6 μM) and 0.8 folds (5.5 μM). These results represent a reduction of about 69% and 91%, respectively of the inflammatory response induced by the cytokines (Fig. 5).

Taken together, these results clearly demonstrated that the main derivatives **1** and **1A** presents significant anti-inflammatory activities, and that the anti-inflammatory properties of **1** are obviously greater than that of **1A**.

2.3. Evaluation of anti-proliferative activities in tumor cells

In this set of experiments, the anti-proliferative activity of the compounds **1** and **1A** in the murine BCa cell line MB49-I was evaluated *in vitro* using the MTT cell viability/proliferation assay as

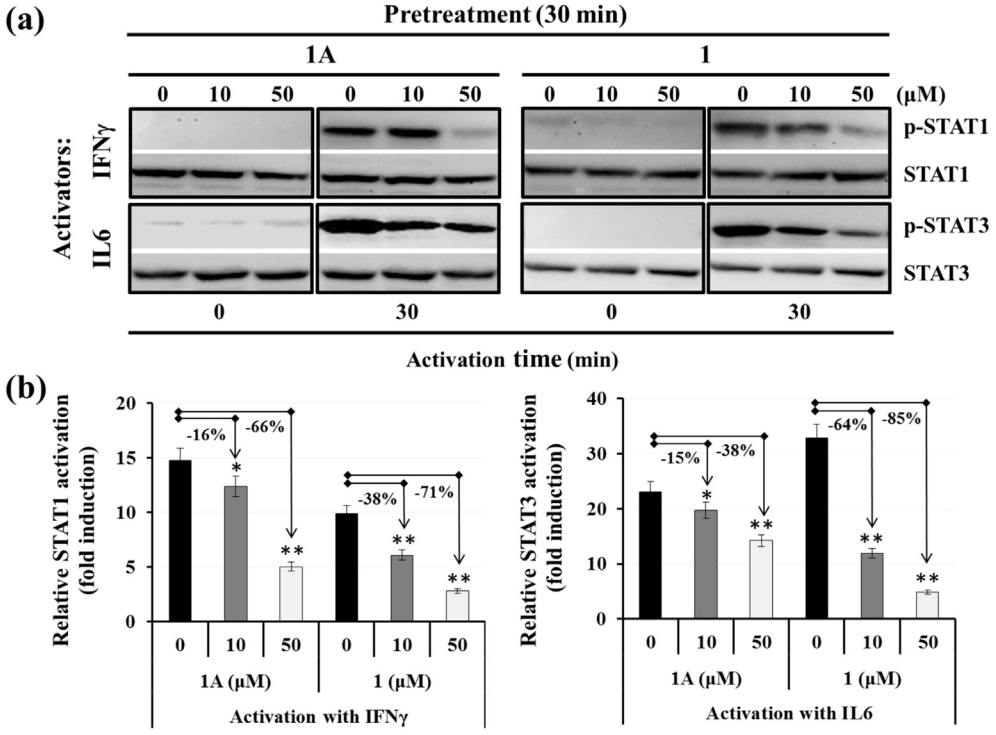

Fig. 2. Representative images (a) and graphical analysis (b) showing the immunodetection of phosphorylated STAT1 and STAT3 in hMϕs pretreated for 30 min with vehicle (DMSO) or compounds **1** and **1A**, and then washed and recovered immediately (t = 0) or after 30 min of activation with either 50 U/mL IFNγ or 25 ng/mL IL6. The ratio of phosphorylated/no phosphorylated proteins was calculated from densitometric analysis of each sample to evaluate the relative activation of pSTAT1 or pSTAT3. $^*p < 0.05$ and $^{**}p < 0.01$ denote significant differences between treatments.

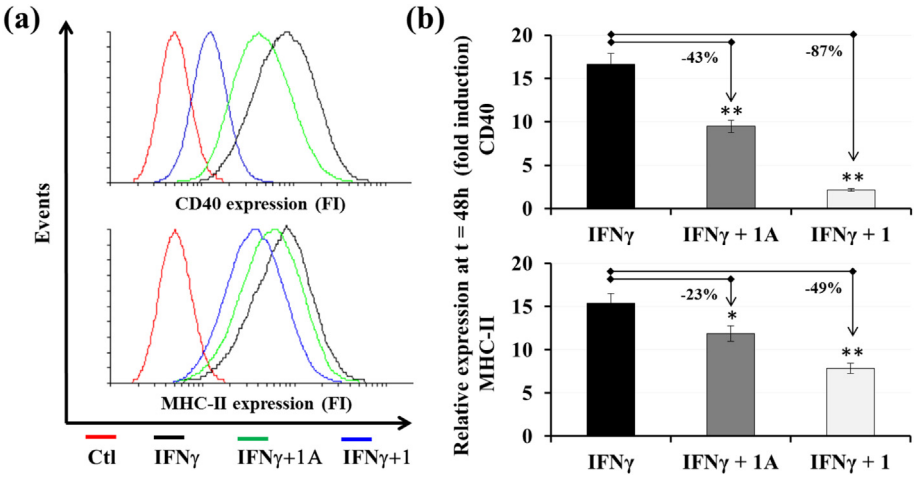

Fig. 3. Representative images (a) and graphical analysis (b) showing flow cytometry analysis to determine the expression level of MHC-II and CD40 surface antigens in resting and IFNγ-activated hMϕs untreated and pretreated with compounds **1** (10 μM) and **1A** (25 μM). $^{*}p < 0.05$ and $^{**}p < 0.01$ denote significant differences between treatments.

previously described [19,20,38,39]. The MTT assay was performed in cells stimulated with INFγ and TNFα, over an incubation period of 24 h, after pretreatment with vehicle (DMSO) and the compounds **1** and **1A**. Relative cell viability data are presented as values of absorbance units (AU) measured at 580 nm. As shown in Fig. 6, derivative **1** was significantly more toxic than its analog **1A**. Indeed, the results demonstrate that pro-inflammatory stimulation inhibits MB49-I cell proliferation, the value of absorbance at t = 24 h being 0.55 AU and 0.35 AU, respectively in the absence and in the presence of INFγ + TNFα stimulation. In INFγ- and TNFα-stimulated cells, derivative **1** is not toxic at a concentration of 10 μM or less but induces a significant reduction in cell proliferation of about 19% at 25 μM, 45% at 37.5 μM and 50% at 50 μM (Fig. 3A). In contrast to **1**, derivative **1A** remains not toxic up to a concentration of 37.5 μM with INFγ + TNFα stimulation (Fig. 6).

2.4. Evaluation of anti-inflammatory properties of the structural components of compound *1*

The next objective of this study was to evaluate individually the anti-inflammatory properties of the various structural components (**MA**, **2**, **3**, **4**, **6**, **7** and **9**, see Scheme 1) of compound **1**. In this set experiments, the various derivatives were tested for their ability to modulate NO production in BCa cells (MB49-I) stimulated by INFγ and TNFα relative to control cells (with cytokines INFγ and TNFα alone). The results found in Fig. 7 show that combined INFγ + TNFα induces an 11-fold increase in the production of NO (from 6 ± 2 μM in unstimulated tumor cells up to 65 ± 7 μM in stimulated tumor

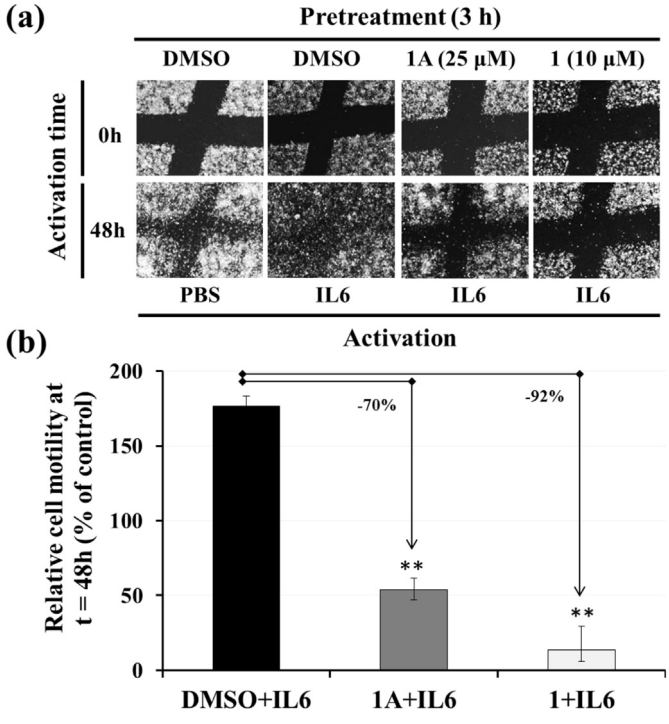

Fig. 4. Representative images (a) and graphical analysis (b) showing scratch wound healing assays performed in hMϕ monolayers cultured for 3 h with vehicle (DMSO) or compounds **1** (10 μM) and **1A** (25 μM), and then activated for 48 h with vehicle (PBS) or 25 ng/mL IL6. The images of the scratch were acquired at t = 0 h and t = 48 h by fluorescence microscopy. Five fields were taken randomly for each different treatment. All observations were performed at 5 × magnification. Cell motility was expressed as percent (%) of control of motile cells at t = 48 h relative to motile cells at t = 0 h $^{*}p < 0.05$ and $^{**}p < 0.01$ denote significant differences between treatments.

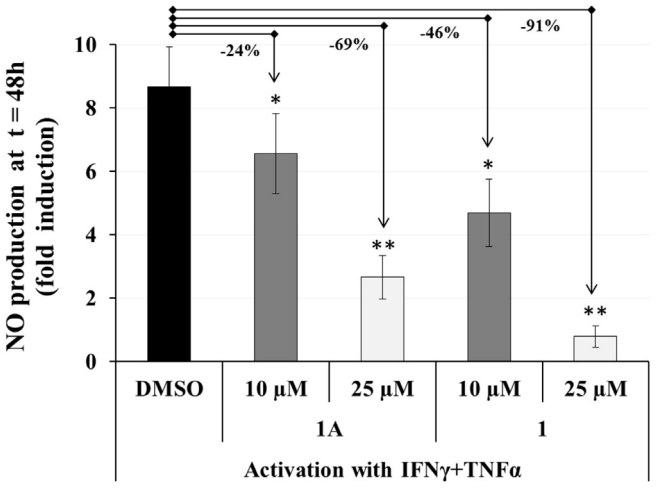

Fig. 5. Graphical representation of NO production in the macrophage-like J774A.1 cells following a pro-inflammatory stimulation by IFNγ and TNFα after pretreatment with vehicle (DMSO) and the derivatives **1** and **1A**. $^{*}p < 0.05$ and $^{**}p < 0.01$ denote significant differences between treatments.

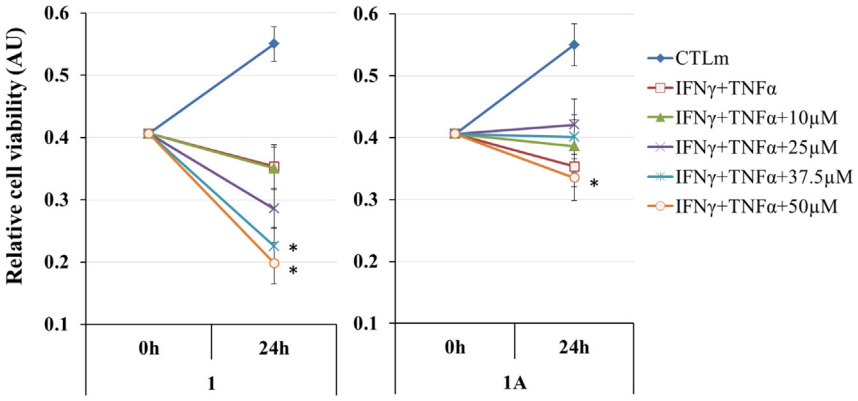

Fig. 6. Graphical representation of relative cell viability on the murine BCa cell line MB49-I following a pro-inflammatory stimulation by IFNγ and TNFα after pretreatment with vehicle (DMSO) and anti-inflammatory derivatives **1** and **1A** at different concentrations. $^{*}p < 0.05$ and $^{**}p < 0.01$ denote significant differences between treatments.

cells). Of note, at a concentration of 50 μM, the induction of NO production was respectively reduced to 2-folds (12 μM) in the presence of **1**, and 4-folds (23 μM) in the presence of **1A**. These results represent a reduction of about 81% and 72%, respectively of the inflammatory response induced by the cytokines. However, it is worth mentioning that the observed reduction of 81% for derivative **1** might be produced by a combination of both cytotoxic and anti-inflammatory activity (see Fig. 6). Also, in the presence of derivatives **1** and **1A** at a concentration of 10 μM, NO production induction was reduced to 7-folds (39 μM) and 9-folds (51 μM), respectively. Interestingly, the reagents **MA** and **2** (PABA) and the synthetic intermediates **3**, **4** and **6** do not present any anti-inflammatory properties (Fig. 7). Furthermore, derivative **7** bearing only the maleimide function (left hand of **1**) and derivative **9** bearing only the *tert*-butyloxycarbonyl function (right hand of **1**) did not show any anti-inflammatory activity (Fig. 7). Hence, the combination of the maleimide function together with the hydrazine amide (either BOC protected (**1**) or as a hydrochloride salt (**1A**)) are necessary for anti-inflammatory activity.

3. Conclusion

In this study, we prepared and characterized several compounds in order to better understand the anti-inflammatory activity of derivatives **1** and **1A**. It is now apparent that the anti-inflammatory activity requires the presence of the maleimide function together with a hydrazine amide function for optimal activity. It is also proven that the various precursor intermediates (**3**, **4**, **6**), reagents (**2**, **PABA**)) and maleic anhydride (**MA**) as well as the left hand (**7**) and right hand (**9**) of the main anti-inflammatory compound **1** were inactive. Significant reductions of STAT1 or STAT3 activation by several pro-inflammatory cytokines were observed with compounds **1** and **1A**. Also, significant decreased of CD40 and MHC-II expressions were observed using **1** and **1A**. Cell motility assays also revealed that **1** and **1A** can induce a drastic reduction of motility as illustrated by a 92% reduction in cell motility at 10 μM for derivative **1**. Relative cell viability revealed that derivative **1A** was less toxic than derivative **1**. Taken together, these results suggest that the development of such type of anti-inflammatory derivative must include the basic carbon skeleton of **1A** as it was proven less toxic that its precursor derivative **1**. Hence, this simple compound might be of interest as a non-toxic anti-inflammatory derivative to investigate the role of inflammation in BCa and other cancers in the future. The results confirm the anti-inflammatory properties of **1**, its analog **1A** and provide an alternative use for **1** that was initially prepared as a heterobifunctional cross-linking

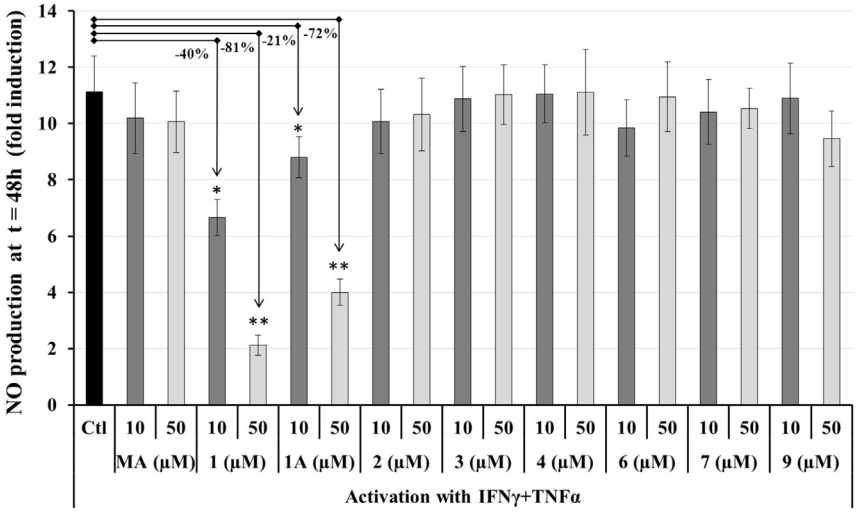

Fig. 7. Graphical representation of NO production by the murine BCa cell line MB49-I following a pro-inflammatory stimulation by IFNγ and TNFα after pretreatment with vehicle (DMSO) and derivatives **1** and **1A** and various precursor intermediates (**3**, **4**, **6**), reagents (**2**, PABA) and maleic anhydride (**MA**) as well as the left hand (**7**) and right hand (**9**) of the main anti-inflammatory compound **1**. $^{*}p < 0.05$ and $^{**}p < 0.01$ denote significant differences between treatments.

reagent. Further studies using an *in vivo* mouse model for BCa invasion and metastasis are currently underway to demonstrate the anticancer effects of these new anti-inflammatory molecules. Once completed, the results from these studies will be reported elsewhere.

4. Experimental protocols

4.1. Biological evaluation

4.1.1. Cell culture

Biological assays were performed using the human monocytic cell line THP1, the murine macrophage-like cell line J774A.1, and the murine BCa cell line MB49-I. The cells were maintained in RPMI medium supplemented with 10% heat-inactivated fetal bovine serum (FBS) and containing 1 mM sodium pyruvate, 10 mM 4-(2-hydroxyethyl)piperazine-1-ethanesulfonic acid (HEPES) and 50 μg/mL gentamycin (referred as 10% FBS RPMI-1640). The cells were maintained at 37 °C in a moisture-saturated atmosphere containing 5% CO_2.

THP1 cells and J774A.1 cells are the most widely used cell lines to investigate the function and differentiation of monocytes and Mϕs in response to various inflammatory mediators [40,41]. Undifferentiated THP1 cells resemble primary monocytes/Mϕs isolated from healthy donors or donors with inflammatory diseases, such as diabetes mellitus and atherosclerosis [42]. After treatment with phorbol esters, THP1 cells differentiate into Mϕ-like cells which mimic native monocyte-derived Mϕs in several respects [43]. As we previously described, green fluorescent protein-expressing (GFP)-THP1 cells were cultured for 18 h in 50 nM phorbol 12-myristate 13-acetate to induce monocyte-to-Mϕ differentiation [19,20,39]. The J774A.1 cell line was kindly provided by Dr Tatiana Scorza (Université du Québec à Montréal, Canada). This cell line is a macrophage-like cell model which produce large amount of NO in response to IFNγ, TNFα, bacterial infection and bacterial products, such as lipopolysaccharide (LPS) [40]. The cell line MB49-I is a highly invasive and tumorigenic BCa cell model that was developed by successive *in vivo* passages of MB49 primary tumors [44].

4.1.2. Cell signaling studies

THP1-derived hMϕs (750×10^3 cells/mL) were pretreated for 30 min with vehicle (DMSO) or compounds **1** and **1A** (both at 10 μM and 50 μM), and then washed and recovered immediately (t = 0 min) or after 30 min of activation with 50 U/mL IFNγ and 25 ng/mL IL6. Cell lysates were prepared and analyzed by immunoblotting as described [19,20,39,45]. Briefly, protein samples were resolved by SDS-PAGE under reducing conditions and transferred onto a PVDF membrane. Blots were first probed with rabbit polyclonal antibodies against phospho-STAT1 (pSTAT1) and pSTAT3 (both at 1:2000) overnight at 4 °C. Blots were then incubated with HRP-conjugated goat anti-rabbit IgG Ab (1:3000) for 1 h at room temperature. The same blots were stripped and then probed with anti-STAT1 and anti-STAT3 Abs (both at 1:1000). In both cases, probed molecules were visualized using an enhancement chemiluminescence detection kit (Thermo Fisher Scientific).

4.1.3. Surface antigen expression analysis

To study membrane receptor expression, THP1-derived hMϕs (750×10^4 cells/mL) were pretreated for 3 h with DMSO or compounds **1** (10 μM) and **1A** (25 μM), and then left untreated (control) or treated for 48 h with 50 U/mL IFNγ. The expression level of MHC-II and CD40 was evaluated by flow cytometry as described [19,20,39].

4.1.4. Motility assays

The *in vitro* scratch wound healing assay was performed to study the effects of compounds **1** (10 μM) and **1A** (25 μM) in IL6-induced hMϕ cell migration, as described [46]. Briefly, THP1-derived hMϕs (750×10^3 cells/mL) were seeded into 24-well tissue culture plate to reach ~70–80% confluence as a monolayer. The cell monolayers were scraped in a straight line in one direction to create a "scratch" with a p200 pipet tip. To obtain the same field during the image acquisition, another straight line was scratched perpendicular to the first would line to create a cross in each well. Cell debris were removed and the edges of the scratch were smoothed by washing the cells once with 1 mL of Hank's buffer. Cell monolayers were pretreated for 3 h with vehicle (DMSO) or compounds **1** (10 μM) and **1A** (25 μM), and then left untreated (control) or treated for 48 h with 25 ng/mL IL6. Using the cross as reference points the plate was placed under an inverted fluorescence microscope, and the images of the scratch were acquired at t = 0 h and t = 48 h. The number of motile cells was determined using Java-based image processing program ImageJ (National Institutes of Health) and relative cell motility was expressed as percent (%) of control of motile cells at t = 48 h relative to motile cells within the initial wound (at t = 0 h).

4.1.5. Evaluation of NO production by the Griess reagent method

The MB49-I cells and the J774A.1 cells (25×10^3 cells/well) were grown and pretreated, as indicated, with various anti-inflammatory derivatives, precursors and mono-functional derivatives for a period of 3 h. Afterwards the cells were washed twice with 10% FBS RPMI-1640 and then activated to produce NO for a period of 24 h with cytokines INFγ and TNFα. NO production was measured using the Griess reagent method as previously described [22]. This method involves the detection of nitrite ions (NO_2^-) formed by the spontaneous oxidation of NO under physiological conditions. According the manufacture procedure (Life Technologies; # G-7921), equal volumes of sulfanilic acid and N-(1-naphthyl)ethylenediamine are mixed together to form the Griess reagent. In the presence of NO_2^-, sulfanilic acid is converted to a diazonium salt, which in turn is coupled to N-(1-naphthyl)ethylenediamine to produce a pink coloration that is measured with a spectrophotometer (Biotek, synergy HT) at 548 nm.

4.1.6. Evaluation of cell proliferation by the MTT assay

To evaluate the anti-proliferative activity, cell viability/proliferation MTT assays were performed as previously described [19,20,38,39,45]. Briefly, MB49-I cells (5×10^3 cells/well) were plated in 96-well plates in 100 μL 10% FBS RPMI-1640 and cultured for 24 h at 37 °C and 5% CO_2. Cells were pretreated for a period of 3 h with vehicle (DMSO) or derivatives **1** and **1A** at 0, 10, 25, 37.5, and 50 μM, and then incubated for 24 h in the absence or the presence of INFγ and TNFα. At the end of the culture period, 10 μL of 5 mg/mL methylthiazolyldiphenyl-tetrazolium bromide (MTT) solution was added to each well. After a 3-h incubation period with MTT reagent, 100 μL of MTT solubilization buffer (10% SDS in 10 mM HCl) was added and plates were placed overnight in the cell incubator before absorbance measure. The optical density was read at 580 nm using the Microplate Reader Manager (from Bio-Rad Laboratories).

4.2. Chemistry

Anhydrous reactions were performed under an inert atmosphere of nitrogen. The starting material, reactant and solvents were obtained commercially and were used as such or purified and dried by standard means [47]. Organic solutions were dried over magnesium sulfate ($MgSO_4$), filtered and evaporated on a rotary evaporator under reduced pressure. All reactions were monitored by UV fluorescence. Commercial TLC plates were Sigma T 6145

(polyester silica gel 60 Å, 0.25 mm). Flash column chromatography was performed according to the method of Still et al. on Merck grade 60 silica gel, 230–400 mesh [48]. All solvents used in chromatography were distilled.

The infrared spectra were taken on a Nicolet Impact 420 FT-IR spectrophotometer. Mass spectral assays were obtained using a MS model 6210, Agilent technology instrument. The high resolution mass spectra (HRMS) were obtained by TOF (time of flight) using ESI (electrospray ionization) using the positive mode (ESI+) (Université du Québec à Montréal). Nuclear magnetic resonance (NMR) spectra were recorded on a Varian 200 MHz NMR apparatus. Samples were dissolved in deuterated acetone (acetone-d_6) or deuterated dimethylsulfoxide (DMSO-d_6) for data acquisition using the residual solvent signal as internal standard (acetone, δ 2.05 ppm for ^{1}H NMR and δ 29.84 ppm for ^{13}C NMR; dimethylsulfoxide, δ 2.50 ppm for ^{1}H NMR and δ 39.52 ppm for ^{13}C NMR). Chemical shifts (δ) are expressed in parts per million (ppm), the coupling constants (J) are expressed in hertz (Hz). Multiplicities are described by the following abbreviations: s for singlet, d for doublet, t for triplet, m for multiplet, #m for several multiplets and, br s for broad singlet.

4.2.1. Synthesis of anti-inflammatory **1** and **1A**

4.2.1.1. Synthesis of derivatives **3**, **4** and **1**.

The synthesis of derivatives **3**, **4** and **1** were performed as described earlier for the same or similar types of compounds [30,31,49,50]. Only, derivatives **4** and **1** were fully characterized earlier [30,31]. So, the spectral data of intermediate **3** and derivative **1A** are given herein. Note: The complete spectral data of **4** and **1** are also provided in order to facilitate the comparision between the various molecules described in this manuscript.

Step 1: Synthesis of 4-(3-carboxy-acryloylamino)-benzoic acid (**3**)

Briefly, *para*-aminobenzoic acid (**2**, 5.34 g, 38.93 mmol) was dissolved in dry acetone (6 mL) to which was added methanol (1 mL). Maleic anhydride (1.05 eq.) dissolved in dry acetone was added to the first solution. The reaction mixture was stirred for a period of 2 h allowing sufficient time for the complete precipitation of the diacid **3**. The precipitate was filtered and washed twice with acetone (2 × 2 mL) and dried in a desiccator overnight. The crude diacid **3** (9.16 g, 90%) was sufficiently pure to be use without further purification at the next step. IR (ν, cm^{-1}): 3500–2500 (CO_2H), 1686 cm^{-1} (C=O); ^{1}H NMR (DMSO-d_6, δ ppm): 12.79 (br s, 2H, 2 × CO_2H), 10.58 (s, 1H, NH), 7.89 and 7.71 (2 × d, J = 8.6 Hz, 4H, aromatic), 6.48 and 6.30 (2 × d, J = 12.2 Hz, 2H, maleimide); ^{13}C NMR (DMSO-d_6, δ ppm): 167.4, 167.3, 164.1, 143.2, 132.1, 130.9 (2), 130.6, 126.0, 119.2 (2); ESI + HRMS: (M + H)+ calculated for $C_{11}H_{10}NO_5$ = 236.0553; found = 236.0558.

Step 2: Synthesis of 4-(2,5-dioxo-2,5-dihydro-pyrrol-1-yl)-benzoic acid (**4**)

The diacid **3** (2.01 g, 8.54 mmol) was treated with acetic anhydride (4.0 mL, 36.28 mmol) and anhydrous sodium acetate (350 mg, 4.27 mmol) and the mixture heated at 50 °C for 2 h. Afterwards, the solution was evaporated to dryness and stirred with water at 70 °C for a period of 2 h. The resulting precipitate was filtered and dried in a desiccator overnight to yield 1.65 g (89%) of maleimide **4**. The spectral data of this derivative correspond to those reported in the literature [30]. IR (ν, cm^{-1}): 3475–2600 (CO_2H), 1715 (C=O), 1704 (C=O); ^{1}H NMR (acetone-d_6, δ ppm): 8.14 and 7.57 (2 × d, J = 8.6 Hz, 4H, aromatic), 7.08 (s, 2H, maleimide); ^{13}C MNR (acetone-d_6, δ ppm) 169.3 (2), 166.2, 136.2, 134.7 (2), 130.1 (2), 129.3, 125.8 (2); ESI + HRMS: (M + H)+ calculated for $C_{11}H_8NO_4$ = 218.0448; found = 218.0447.

Step 3: Synthesis of *N*′-[4-(2,5-dioxo-2,5-dihydro-pyrrol-1-yl)-benzoyl]-hydrazinecarboxylic acid *tert*-butyl ester (**1**)

Derivative **1** was synthesized using a modified procedure reported by Willner et al. [51] as it is also described by Lau et al. [31]. A cooled suspension (0 °C) of molecule **4** (211 mg, 0.97 mmol) in methylene chloride (4.5 mL) was treated with triethylamine (190 μL, 1.36 mmol) and isobutyl chloroformate (175 μL, 1.34 mmol). The mixture was stirred for 1 h at 0 °C and at room temperature (22 °C) for about 1 h. Afterwards, *tert*-butyl carbazate (128 mg, 0.97 mmol) dissolved in methylene chloride (0.8 mL) was added dropwise to the mixture and stirred for an additional 12 h at 22 °C. The reaction mixture was diluted with ethyl acetate (55 mL) and methylene chloride (20 mL) and washed twice with saturated $NaHCO_3$ (2 × 50 mL), twice with 0.1 N HCl (2 × 50 mL), twice with saturated NaCl (2 × 50 mL), and finally with H_2O (50 mL). The organic phase was dried ($MgSO_4$) and evaporated to give crude derivative **1**. The product was purified by flash chromatography, using a mixture of hexanes/acetone (3/2), to yield 173 mg (54%) of **1**. The spectral data of this derivative correspond to those reported in the literature [31]. IR (ν, cm^{-1}): 3360–3240 (NH), 3087 (C=C), 2988 (CH, aliphatic), 1733 (C=O), 1706 (C=O). ^{1}H NMR (acetone-d_6, δ ppm): 9.05 (s, 1H, NH), 8.02 and 7.53 (2 × d, J = 8.6 Hz, 4H, aromatic), 7.07 (s, 2H, maleimide), 2.84 (br s, 1H, NH), 1.45 (s, 9H, 3 × CH_3); ^{13}C RMN (acetone-d_6, δ ppm): 169.3 (2), 166.0, 155.7, 135.1, 134.6 (2), 131.6, 127.9 (2), 125.9 (2), 79.6, 27.5 (3); ESI + HRMS: (M + Na)+ calculated for $C_{16}H_{17}N_3NaO_5$ = 354.1060; found = 354.1072; (M -2-methylpropene + H)+ calculated for $C_{12}H_{11}N_3O_5$ = 276.0620; found = 276.0627.

4.2.1.2. Synthesis of derivative 4-(2,5-dioxo-2,5-dihydro-pyrrol-1-yl)-benzoic acid hydrazide hydrochloride (**1A**).

The hydrolysis of **1** was performed using a similar procedure reported by Heindel et al. for the cleavage of maleimidoacetic acid (*tert*-butyloxycarbonyl) hydrazide with hydrochloric acid to form maleimidoacetic acid hydrazide hydrochloride [52]. To a solution of **1** (2.41 g, 7.27 mmol) dissolved in dry dioxane (30 mL) was added a solution of hydrochloric acid (60 mL, 1.0 M in diethyl ether, 60 mmol). The mixture was stirred at room temperature for a period of 5 h. Afterwards, 150 mL of hexanes were added to complete the precipitation of the hydrochloride salt **1A**. The crude precipitated was filtered, washed with hexanes and recrystallized twice with a mixture of methanol/isopropyl alcohol/hexanes (8/3/10) to yield 1.7 g (46%) of the desired material. IR (ν, cm^{-1}): 3200–2500 (CO_2H), 3269 (NH), 1702 (C=O), 1693 (C=O); ^{1}H NMR (DMSO-d_6, δ ppm): 8.06 and 7.52 (2 × d, J = 8.8 Hz, 4H, aromatic), 7.21 (s, 2H, maleimide); ^{13}C MNR (DMSO-d_6, δ ppm) 170.0 (2), 165.6, 135.9, 135.4 (2), 129.6, 129.0 (2), 126.8 (2); ESI + HRMS: (M + H)+ calculated for $C_{11}H_{10}N_3O_3$ = 232.0717; found = 232.0717 and ESI + HRMS: (M + H)+ calculated for $C_{11}H_{11}ClN_3O_3$ = 268.0483; found = 268.0483.

4.2.2. Synthesis of derivatives **6**.**7** and **9**

4.2.2.1. Synthesis of derivative **7**

Step 1: Synthesis of 3-phenylcarbamoyl-acrylic acid (**6**)

Following the procedure described earlier for the preparation of derivative **3** using aniline (3.0 g, 2.96 mL, 32.4 mmol), MA (3.33 g, 34.0 mmol) and dry acetone (21 mL). The precipitated was filtered and washed with dry acetone (2 × 3 mL) and dried in a desiccator overnight. The reaction yielded acid **6** (5.36 g, 86%) that was used as

such in the next step. IR (ν, cm^{-1}): 3273 and 3208 (N–H), 3230–2900 (CO_2H), 1694 cm^{-1} (C=O); ^1H NMR (DMSO-d_6, δ ppm): 12.87 (br s, 1H, CO_2H), 10.37 (s, 1H, NH), 7.60, 7.31 and 7.07 (3 × m, 2H, 2H and 1H, aromatic), 6.46 and 6.28 (2 × d, J = 12.1 Hz, 2H, maleimide); ^{13}C NMR (DMSO-d_6, δ ppm): 167.3, 163.7, 139.0, 132.1, 130.9, 129.3 (2), 124.3, 120.0 (2); ESI + HRMS: (M + H)+ calculated for $C_{10}H_{10}NO_3$ = 192.0655; found = 192.0650.

Step 2: Synthesis of 1-phenyl-pyrrole-2,5-dione (**7**)

Following the procedure described above for the preparation of derivative **4** using acid **6** (823 mg, 4.28 mmol), acetic anhydride (2.10 mL, 22.2 mmol), sodium acetate (175 mg, 2.13 mmol), 50 °C for 2 h, then H_2O (80 mL), 70 °C for 2 h. The final product was filtered, dried overnight in a desiccator to give 325 mg (44%) of final product. This compound is also commercially available from Sigma–Aldrich Inc. IR (ν, cm^{-1}): 1703 (C=O); ^1H NMR (acetone-d_6, δ ppm): 7.75, 7.34 and 7.13 (3 × m, 2H, 2H and 1H, aromatic), 6.43 (s, 2H, maleimide); ^{13}C MNR (acetone-d_6, δ ppm) 163.1 (2), 138.7, 133.4 (2), 128.8 (2), 124.2, 119.8 (2); ESI + HRMS: (M + H)+ calculated for $C_{10}H_8NO_2$ = 174.0550; found = 174.0554.

*4.2.2.2. Synthesis of derivative N′-benzoyl-hydrazinecarboxylic acid tert-butyl ester (**9**).* Following the procedure described earlier for the preparation of derivative **1** using benzoic acid (321 mg, 2.62 mmol), triethylamine (513 μL, 3.68 mmol), isobutyl chloroformate (480 μL, 3.68 mmol), *tert*-butyl carbazate (347 mg, 2.62 mmol) and methylene chloride (8 mL in total). The crude material was purified by flash chromatography using a mixture of hexanes/ethyl acetate (9/1 and 7/3) to yield the desired material **9** (300 mg, 48%). IR (ν, cm^{-1}): 3475–3150 (NH), 3070 (C=C), 2979 (CH, aliphatic), 1713 (C=O), 1659 (C=O). ^1H NMR (acetone-d_6, δ ppm): 9.43 (s, 1H, NH), 7.92 and 7.50 (2 × m, 5H, aromatic), 2.84 (br s, 1H, NH), 1.44 (s, 9H, 3 × CH_3); ^{13}C RMN (acetone-d_6, δ ppm): 166.5, 155.7, 133.1, 131.7, 128.4 (2), 127.3 (2), 79.5, 27.5 (3); ESI + HRMS: (M + Na)+ calculated for $C_{12}H_{16}N_2NaO_3$ = 259.1053; found = 259.1058; (M -2-methylpropene + H)+ calculated for $C_8H_9N_2O_3$ = 181.0613; found = 181.0612.

4.3. Statistical analyses

For all biological assays, data were presented as mean ± SD from three independent experiments. Data were analyzed by one-way ANOVA followed by Bonferonni post-test using Prism software, version 3.03 (GraphPad, San Diego, CA). *p* values of ≤0.05 were considered to indicate statistical significance.

Acknowledgments

This work was supported by grants from the Natural Sciences and Engineering Research Council of Canada (NSERC #2014-06516), the Fonds Québécois de la Recherche sur la Nature et les Technologies (FQRNT), and the Réseau Québécois en Reproduction (RQR) to C. Reyes-Moreno. S. Cloutier is a recipient of a NSERC undergraduate summer scholarship award. J. Hamelin-Morrissette is supported by the RQR-CREATE scholarships program. J. Girouard holds a postdoctoral fellowship from the Fonds de la Recherche en Santé du Québec (FRSQ). D. Belgorosky holds a doctoral scholarship from the Emerging Leaders in the Americas Program from Canada.

References

[1] R.L. Siegel, K.D. Miller, A. Jemal, Cancer statistics, 2015, CA: A Cancer J. Clin. 65 (2015) 5–29.
[2] Canadian Cancer Society's Advisory Committee on Cancer Statistics, Canadian Cancer Statistics 2014, Canadian Cancer Society, Toronto, ON, 2014.
[3] S. Brandau, H. Suttmann, Thirty years of BCG immunotherapy for non-muscle invasive bladder cancer: a success story with room for improvement, Biomed. Pharmacother. 61 (2007) 299–305.
[4] S.J. Dovedi, B.R. Davies, Emerging targeted therapies for bladder cancer: a disease waiting for a drug, Cancer metastasis Rev. 28 (2009) 355–367.
[5] D.B. Thompson, L.E. Siref, M.P. Feloney, R.J. Hauke, D.K. Agrawal, Immunological basis in the pathogenesis and treatment of bladder cancer, Expert Rev. Clin. Immunol. 11 (2015) 265–279.
[6] Z. Zhu, Z. Shen, C. Xu, Inflammatory pathways as promising targets to increase chemotherapy response in bladder cancer, Mediat. Inflamm. 2012 (2012) 528690.
[7] D.S. Michaud, Chronic inflammation and bladder cancer, Urol. Oncol. 25 (2007) 260–268.
[8] A. Ben-Baruch, Inflammation-associated immune suppression in cancer: the roles played by cytokines, chemokines and additional mediators, Semin. Cancer Biol. 16 (2006) 38–52.
[9] L.M. Coussens, Z. Werb, Inflammation and cancer, Nature 420 (2002) 860–867.
[10] F. Colotta, P. Allavena, A. Sica, C. Garlanda, A. Mantovani, Cancer-related inflammation, the seventh hallmark of cancer: links to genetic instability, Carcinogenesis 30 (2009) 1073–1081.
[11] A.F. Kantor, P. Hartge, R.N. Hoover, A.S. Narayana, J.W. Sullivan, J.F. Fraumeni Jr., Urinary tract infection and risk of bladder cancer, Am. J. Epidemiol. 119 (1984) 510–515.
[12] C. La Vecchia, E. Negri, B. D'Avanzo, R. Savoldelli, S. Franceschi, Genital and urinary tract diseases and bladder cancer, Cancer Res. 51 (1991) 629–631.
[13] D.L. Lamm, R.F. Gittes, Inflammatory carcinoma of the bladder and interstitial cystitis, J. Urol. 117 (1977) 49–51.
[14] T. Cai, S. Mazzoli, F. Meacci, G. Tinacci, G. Nesi, E. Zini, R. Bartoletti, Interleukin-6/10 ratio as a prognostic marker of recurrence in patients with intermediate risk urothelial bladder carcinoma, J. Urol. 178 (2007) 1906–1911 discussion 1911–1902.
[15] S. Brandau, Tumor associated macrophages: predicting bacillus Calmette-Guerin immunotherapy outcomes, J. Urol. 181 (2009) 1532–1533.
[16] T. Hanada, M. Nakagawa, A. Emoto, T. Nomura, N. Nasu, Y. Nomura, Prognostic value of tumor-associated macrophage count in human bladder cancer, Int. J. Urol. 7 (2000) 263–269.
[17] C. Ayari, H. LaRue, H. Hovington, M. Decobert, F. Harel, A. Bergeron, B. Tetu, L. Lacombe, Y. Fradet, Bladder tumor infiltrating mature dendritic cells and macrophages as predictors of response to bacillus Calmette-Guerin immunotherapy, Eur. Urol. 55 (2009) 1386–1395.
[18] H. Takayama, K. Nishimura, A. Tsujimura, Y. Nakai, M. Nakayama, K. Aozasa, A. Okuyama, N. Nonomura, Increased infiltration of tumor associated macrophages is associated with poor prognosis of bladder carcinoma in situ after intravesical bacillus Calmette-Guerin instillation, J. Urol. 181 (2009) 1894–1900.
[19] M. Dufresne, G. Dumas, E. Asselin, C. Carrier, M. Pouliot, C. Reyes-Moreno, Pro-inflammatory type-1 and anti-inflammatory type-2 macrophages differentially modulate cell survival and invasion of human bladder carcinoma T24 cells, Mol. Immunol. 48 (2011) 1556–1567.
[20] G. Dumas, M. Dufresne, E. Asselin, J. Girouard, C. Carrier, C. Reyes-Moreno, CD40 pathway activation reveals dual function for macrophages in human endometrial cancer cell survival and invasion, Cancer Immunol. Immunother. 62 (2013) 273–283.
[21] B.B. Aggarwal, R.V. Vijayalekshmi, B. Sung, Targeting inflammatory pathways for prevention and therapy of cancer: short-term friend, long-term foe, Clinical Cancer Research: Official J. Am. Assoc. Cancer Res. 15 (2009) 425–430.
[22] D. Belgorosky, Y. Langle, B. Prack Mc Cormick, L. Colombo, E. Sandes, A.M. Eijan, Inhibition of nitric oxide is a good therapeutic target for bladder tumors that express iNOS, Nitric Oxide 36 (2014) 11–18.
[23] A.J. Burke, F.J. Sullivan, F.J. Giles, S.A. Glynn, The yin and yang of nitric oxide in cancer progression, Carcinogenesis 34 (2013) 503–512.
[24] S.P. Hussain, P. He, J. Subleski, L.J. Hofseth, G.E. Trivers, L. Mechanic, A.B. Hofseth, M. Bernard, J. Schwank, G. Nguyen, E. Mathe, D. Djurickovic, D. Haines, J. Weiss, T. Back, E. Gruys, V.E. Laubach, R.H. Wiltrout, C.C. Harris, Nitric oxide is a key component in inflammation-accelerated tumorigenesis, Cancer Res. 68 (2008) 7130–7136.
[25] I. Jung, E. Messing, Molecular mechanisms and pathways in bladder cancer development and progression, Cancer Control: J. Moffitt Cancer Cent. 7 (2000) 325–334.
[26] E.O. Sandes, C. Lodillinsky, Y. Langle, D. Belgorosky, L. Marino, L. Gimenez, A.R. Casabe, A.M. Eijan, Inducible nitric oxide synthase and PPARgamma are involved in bladder cancer progression, J. Urol. 188 (2012) 967–973.
[27] D. Vasudevan, D.D. Thomas, Insights into the diverse effects of nitric oxide on tumor biology, Vitam. Horm. 96 (2014) 265–298.
[28] M. Coimbra, S.A. Kuijpers, S.P. van Seters, G. Storm, R.M. Schiffelers, Targeted delivery of anti-inflammatory agents to tumors, Curr. Pharm. Des. 15 (2009) 1825–1843.
[29] W.-S. Choi, P.-Y. Shin, J.-H. Lee, G.-D. Kim, The regulatory effect of veratric acid on NO production in LPS-stimulated RAW264.7 macrophage cells, Cellular Immunol. 280 (2012) 164–170.
[30] A. Lau, G. Berube, C.H. Ford, Conjugation of doxorubicin to monoclonal anti-carcinoembryonic antigen antibody via novel thiol-directed cross-linking reagents, Bioorg. Med. Chem. 3 (1995) 1299–1304.

[31] A. Lau, G. Berube, C.H. Ford, M. Gallant, Novel doxorubicin-monoclonal anti-carcinoembryonic antigen antibody immunoconjugate activity in vitro, Bioorg. Med. Chem. 3 (1995) 1305–1312.
[32] U. Boehm, T. Klamp, M. Groot, J.C. Howard, Cellular responses to interferon-gamma, Annu. Rev. Immunol. 15 (1997) 749–795.
[33] S.M. Hurst, T.S. Wilkinson, R.M. McLoughlin, S. Jones, S. Horiuchi, N. Yamamoto, S. Rose-John, G.M. Fuller, N. Topley, S.A. Jones, Il-6 and its soluble receptor orchestrate a temporal switch in the pattern of leukocyte recruitment seen during acute inflammation, Immunity 14 (2001) 705–714.
[34] Z. Xing, J. Gauldie, G. Cox, H. Baumann, M. Jordana, X.F. Lei, M.K. Achong, IL-6 is an antiinflammatory cytokine required for controlling local or systemic acute inflammatory responses, J. Clin. Invest 101 (1998) 311–320.
[35] P.C. Heinrich, I. Behrmann, S. Haan, H.M. Hermanns, G. Muller-Newen, F. Schaper, Principles of interleukin (IL)-6-type cytokine signalling and its regulation, Biochem. J. 374 (2003) 1–20.
[36] T. Clahsen, F. Schaper, Interleukin-6 acts in the fashion of a classical chemokine on monocytic cells by inducing integrin activation, cell adhesion, actin polymerization, chemotaxis, and transmigration, J. Leukoc. Biol. 84 (2008) 1521–1529.
[37] D. Frankova, Z. Zidek, IFN-gamma-induced TNF-alpha is a prerequisite for in vitro production of nitric oxide generated in murine peritoneal macrophages by IFN-gamma, Eur. J. Immunol. 28 (1998) 838–843.
[38] J. Carmichael, W.G. DeGraff, A.F. Gazdar, J.D. Minna, J.B. Mitchell, Evaluation of a tetrazolium-based semiautomated colorimetric assay: assessment of chemosensitivity testing, Cancer Res. 47 (1987) 936–942.
[39] A. Dallagi, J. Girouard, J. Hamelin-Morrissette, R. Dadzie, L. Laurent, C. Vaillancourt, J. Lafond, C. Carrier, C. Reyes-Moreno, The activating effect of IFN-gamma on monocytes/macrophages is regulated by the LIF-trophoblast-IL-10 axis via Stat1 inhibition and Stat3 activation, Cell. Mol. Immunol. (2014) 1–16.
[40] S. Lemaire, M.P. Mingeot-Leclercq, P.M. Tulkens, F. Van Bambeke, Study of macrophage functions in murine J774 cells and human activated THP-1 cells exposed to oritavancin, a lipoglycopeptide with high cellular accumulation, Antimicrob. Agents Chemother. 58 (2014) 2059–2066.
[41] J. Auwerx, The human leukemia cell line, THP-1: a multifacetted model for the study of monocyte-macrophage differentiation, Experientia 47 (1991) 22–31.
[42] Z. Qin, The use of THP-1 cells as a model for mimicking the function and regulation of monocytes and macrophages in the vasculature, Atherosclerosis 221 (2012) 2–11.
[43] M. Daigneault, J.A. Preston, H.M. Marriott, M.K. Whyte, D.H. Dockrell, The identification of markers of macrophage differentiation in PMA-stimulated THP-1 cells and monocyte-derived macrophages, PloS One 5 (2010) 0008668.
[44] V.T. Fabris, C. Lodillinsky, M.B. Pampena, D. Belgorosky, C. Lanari, A.M. Eijan, Cytogenetic characterization of the murine bladder cancer model MB49 and the derived invasive line MB49-I, Cancer Genet. 205 (2012) 168–176.
[45] K. Leduc, V. Bourassa, E. Asselin, P. Leclerc, J. Lafond, C. Reyes-Moreno, Leukemia inhibitory factor regulates differentiation of trophoblast-like BeWo cells through the activation of JAK/STAT and MAPK3/1 MAP Kinase-signaling pathways, Biol. Reprod. 86 (2012) 1–10.
[46] M.B. Menon, N. Ronkina, J. Schwermann, A. Kotlyarov, M. Gaestel, Fluorescence-based quantitative scratch wound healing assay demonstrating the role of MAPKAPK-2/3 in fibroblast migration, Cell. Motil. Cytoskelet. 66 (2009) 1041–1047.
[47] B. Wiemer, D.D. Perrin, W.L.F. Armarego, Purification of Laboratory Chemicals. 3. Aufl., 1988, 391 S., ISBN 0-08-034714-2, in: Acta hydrochimica et hydrobiologica, vol. 17, Pergamon Press, Oxford, 1989, 632–632.
[48] W.C. Still, M. Kahn, A. Mitra, Rapid chromatographic technique for preparative separations with moderate resolution, J. Org. Chem. 43 (1978) 2923–2925.
[49] S. Yoshitake, Y. Yamada, E. Ishikawa, R. Masseyeff, Conjugation of glucose oxidase from *Aspergillus niger* and rabbit antibodies using *N*-hydroxysuccinimide ester of N-(4-carboxycyclohexylmethyl)-maleimide, Eur. J. Biochem. 101 (1979) 395–399.
[50] P. Hermentin, R. Doenges, P. Gronski, K. Bosslet, H.P. Kraemer, D. Hoffmann, H. Zilg, A. Steinstraesser, A. Schwarz, L. Kuhlmann, et al., Attachment of rhodosaminylanthracyclinone-type anthracyclines to the hinge region of monoclonal antibodies, Bioconjug. Chem. 1 (1990) 100–107.
[51] D. Willner, P.A. Trail, S.J. Hofstead, H.D. King, S.J. Lasch, G.R. Braslawsky, R.S. Greenfield, T. Kaneko, R.A. Firestone, (6-Maleimidocaproyl)hydrazone of doxorubicin. A new derivative for the preparation of immunoconjugates of doxorubicin, Bioconjug. Chem. 4 (1993) 521–527.
[52] N.D. Heindel, H.R. Zhao, R.A. Egolf, C.H. Chang, K.J. Schray, J.G. Emrich, J.P. McLaughlin, D.V. Woo, A novel heterobifunctional linker for formyl to thiol coupling, Bioconjug. Chem. 2 (1991) 427–430.